An altitude-normalized magnetic map of Mars and its interpretation

M. Purucker [1], D. Ravat [2], H. Frey [3], C. Voorhies [3], T. Sabaka [4], M. Acuña [5]

Abstract. Techniques developed for the reduction and analysis of terrestrial satellite magnetic field data are used to better understand the magnetic field observations made by Mars Global Surveyor. A global distribution of radial (B_r) magnetic field observations and associated uncertainties is inverted for an equivalent source magnetization distribution and then used to generate an altitude- normalized map of B_r at 200 km. The observations are well-represented by a potential function of crustal origin, consistent with a remanent origin for the Martian magnetic features. The correlation between the 40546 B_r observations and B_r calculated from the magnetization solution at observation locations is 0.978. For a magnetization distribution confined to a 50 km layer, calculated magnetizations range from -22 to +17 A/m. We see correlations with tectonics that were only hinted at in earlier maps. Magnetic features appear to be truncated against Valles Marineris and Ganges Chasma, suggestive of a major change in crustal properties associated with faulting.

Introduction

On the basis of their coherence in a Mars-centered coordinate system and because of their small spatial scale, *Acuña et al.* [1999] interpreted the magnetic field observations during the aerobraking phase of Mars Global Surveyor (MGS) as originating in the Martian crust. In this paper we test the assertion that the majority of the magnetic signal arises from magnetic remanence carried in the Martian crust. We then interpret an altitude-normalized map of the magnetic field, much as we do for Earth, by comparing the map with Mars' geology, geophysics, and topography. On Earth, magnetic field observations are used for structural geologic reconstructions [*Blakely et al.*, 1995]; we expect they may have similar utility on Mars.

The Observations

The dual vector fluxgate magnetometers on the MGS solar panels are limited by residual spacecraft fields to an est-

[1]Raytheon ITSS at Geodynamics Branch, Goddard Space Flight Center, Greenbelt, Maryland

[2]Dept. of Geology, Southern Illinois University, Carbondale, Illinois

[3]Geodynamics Branch, NASA, Goddard Space Flight Center, Greenbelt, Maryland

[4]Raytheon ITSS at Geodynamics Branch, Goddard Space Flight Center, Greenbelt, Maryland

[5]Planetary Magnetospheres Branch, NASA, Goddard Space Flight Center, Greenbelt, Maryland

imated accuracy of 3 nT [*Acuña et al.*, 1999]. For this study, we restrict attention to observations acquired below 200 km altitude to better detect crustal fields. Observations at these altitudes were acquired during both aerobraking phases of the mission (AB1 and AB2 in 1998-1999) and during the science phasing orbits (SPO-1 and SPO-2 in 1998). *Acuña* [2000] has recently made binned AB data available. This data was averaged over equiangular 3-dimensional blocks of 1 degree by 1 degree by 10 km in longitude, latitude, and altitude, respectively. The altitude range is 80 to 200 km and is defined with respect to a sphere of radius 3393.5 km. Latitude coverage ranges from 87°S to 78°N latitude. The magnetic field data (B_r,B_θ,B_ϕ) are given in a spherical coordinate system with B_r defined positive outward, B_θ southward, and B_ϕ eastward. Standard deviations are calculated for all bins with 3 or more vector measurements. Bins with less than 3 observations are not included in the solution reported here. The AB data were collected at all local times but are dominated by dayside observations. The SPO data were preprocessed in the same way as the AB data, but the altitude range is 150 to 200 km. Latitude coverage ranges from 47°N to 86°N, with a preponderance of data poleward of 60°. There are 40546 bins with more than 3 observations, some 30100 of which are from the AB phase of the MGS mission.

The Method

We reduce magnetic field observations to a common altitude via an intermediate step in which we fit n irregularly distributed vector magnetic field observations to an icosahedral mesh of m dipoles [*Purucker et al.*, 1996]. This equivalent source technique represents a magnetic field as

$$\tilde{b} = \tilde{D}x + \tilde{\nu}, \tag{1}$$

where $\tilde{b}$ is the vector containing the magnetic field observations, x is the vector containing the dipole moments to be determined, $\tilde{D}$ is the geometric source function matrix relating x to $\tilde{b}$, and $\tilde{\nu}$ is the observation noise vector (assumed random) of mean zero and covariance W^{-1}. To normalize $\tilde{\nu}$, we pre-multiply (1) by $W^{1/2}$:

$$b = Dx + \nu. \tag{2}$$

We seek to minimize $L(x) = \nu^T \nu$, which leads to the corresponding normal equations:

$$D^T D x = D^T b. \tag{3}$$

The dipoles are located at the surface of a reference sphere of radius 3393.5 km. Because the magnetic field decays rapidly with distance, we exploit the sparseness of the n by m design matrix D numerically by using a preconditioned conjugate gradient approach to determine the dipole
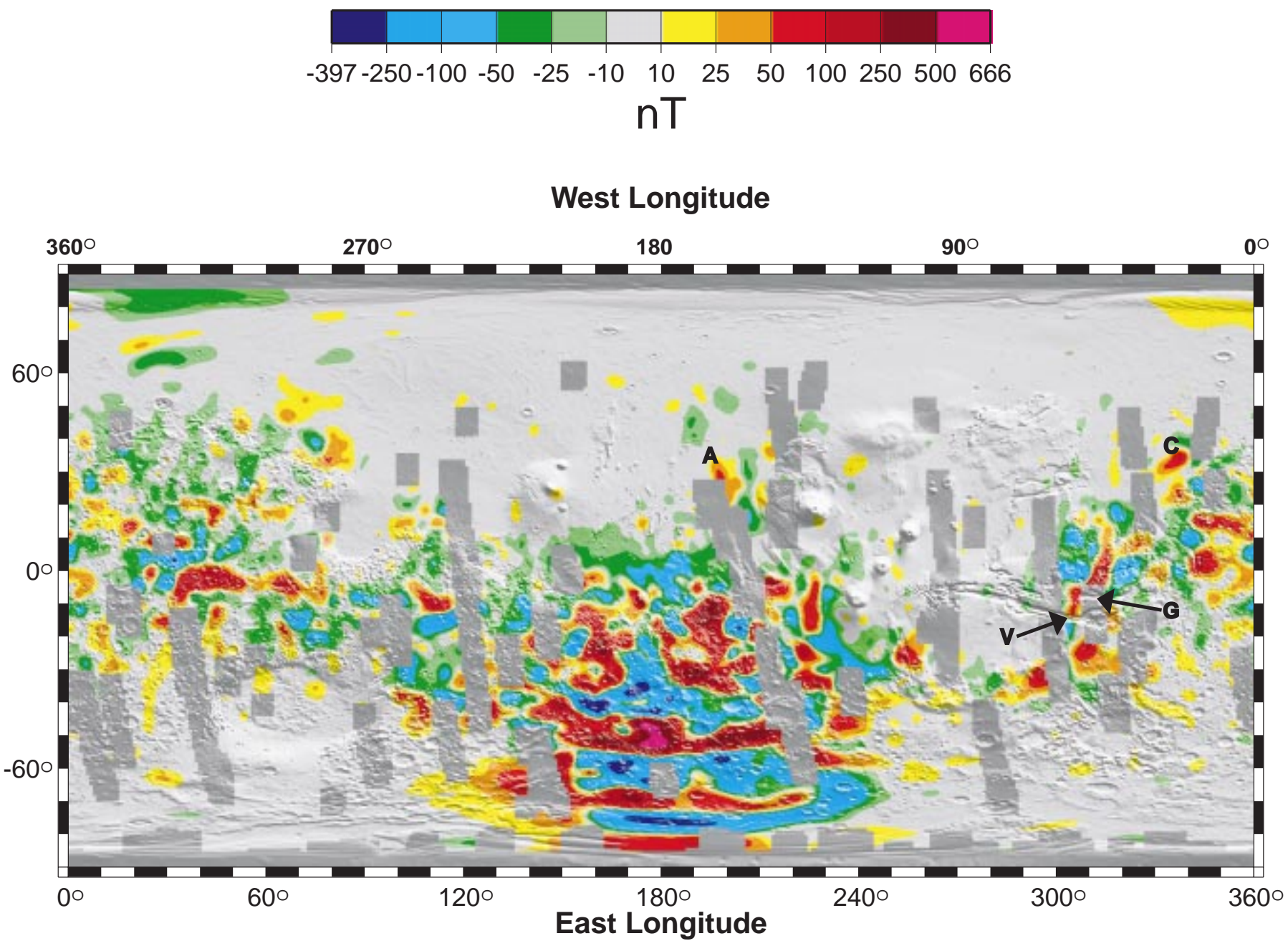
Plate 1. Radial magnetic field (B_r) computed at 200 km altitude in color, overlain on gray-shaded topographic gradient map of Mars (MOLA data). The dark grey bands show regions of inadequate data coverage. The magnetic features are at multiple scales, as evidenced by the logarithmic color scale. V locates the truncated magnetic feature at Valles Marineris, G at Ganges Chasm. A and C indicate magnetic features in young terrain west of Olympus Mons (A) and in eastern Chryse Planitia (C).

moments. The preconditioner divides each row by the L_1 norm of that row. These magnetizations are used to calculate the field at 200 km altitude on a regular grid. Our dipole basis consists of 11550 dipoles spaced in an approximately equal-area fashion, with average spacing of 111 km (1.89°). The dipoles cover the region between 86.5°N and S latitudes and are oriented radially. An equivalent source approach can also be utilized to solve for magnetization directions. We did not do so because it would require three times the computational resources and would make only second-order changes to the resulting altitude-normalized magnetic field map.

The design matrix D includes elements only where the observation to dipole distance is less than 1500 km. This has been found experimentally to yield a solution for x very similar to that using the full D matrix for Earth [*Purucker et al.*, 1996] and Mars is a smaller planet. We do not explicitly form the normal matrix $D^T D$, but rather use matrix identities to reduce the task to two multiplications of D by a vector.

The equivalent source solution x is derived from B_r and associated standard deviations in bins with more than three observations. We use radial in preference to horizontal components because B_r shows the least contribution from external fields [*Acuña et al.*, 1999]. The conjugate gradient method was terminated after 87 iterations, when the root mean square weighted residual

$$\sigma_k = \sqrt{\frac{(b - Dx_k)^T (b - Dx_k)}{n}} \qquad (4)$$

calculated after each iteration k, was no longer decreasing.

Results

The radial magnetic component calculated at 200 km altitude from this solution is shown in Plate 1. Weighted residuals, or misfits $b - Dx$, are least in regions where magnetic features exhibit the largest amplitude and vice-versa. This pattern holds true for all altitudes and there is no change in misfit with altitude.

For $|B_r| > 50$ nT, 69 % of the observations are fitted to within 2σ. For fields exceeding 25 (10) nT, 63 % (52 %) of the observations are so fitted. The larger than expected misfits may be in part due to 1) assignment of the bin location to the center of the bin instead of the true mean measurement location, and 2) unmodeled external fields. Interpreters should thus treat with caution the 10 nT color level on Plate 1.

A global measure of the ability of the solution to match the observations is the 0.978 coefficient of correlation between the observations b and B_r calculated from the solution at the observation locations.

There is also a tendency for the weighted residuals to be positive at high southern latitudes and negative in the northern hemisphere. This might be interpreted as the signature of an external dipole with a q_1^0 of about 4 nT. The origin of this feature is still unmodeled but it is most likely associated with a current system resulting from the Mars-solar wind interaction.

We have also upwardly continued the solution to an altitude of 400 km, where calculated B_r ranges from -107 to +197 nT. These magnitudes compare well with preliminary data acquired from the MGS mapping orbit of 380 km. They can also be compared with the crustal component of terrestrial B_r observations at 400 km, which range from -18 to +21 nT [*Purucker et al.*, 1996]. The maximum Martian magnetic field is therefore some 8 times greater than the terrestrial magnetic field of crustal origin. However, the terrestrial magnetic field originating in the core masks the crustal magnetic field at the longest wavelengths.

The spatial magnetic power spectrum for Mars, computed through spherical harmonic degree 90 from the solution shown in Plate 1, shows no sign of a core-source field. However, the observed spectrum can be fitted by the crustal spectrum expected from random polarity dipoles at a depth of about 50 km below the reference sphere. This depth does not imply the thickness of the magnetic layer, a quantity which remains unknown.

Interpretation and Discussion

The measured magnetic signal represents the product of a magnetization times a layer thickness. The layer thickness on Earth is the depth to the Curie point, typically about 40 km under the continents. On Mars, modeling of gravity and topographic data by *Zuber et al.* [2000] suggests an average crustal thickness of 50 km. Assuming that the dipoles represent crustal elements some 50 km thick, the range of magnetizations determined is -22 to +17 A/m.

If the true magnetizations are predominantly radial, then the B_r fields will be centered over their sources and the steepest gradients will correspond to the boundaries between magnetic elements. If the true magnetizations are dominantly horizontal, the B_r fields will be offset from their sources. Assuming a radial magnetization (as done here) tends to minimize the required magnetizations but makes only small changes to the B_r map at 200 km. Inversions done using horizontal dipoles require maximum magnetizations 2-3 times greater than those done using radial dipoles and do not fit the data as well.

The apparent truncation of a long, N-S, linear and arcuate positive B_r feature (V on Plate 1) at the eastern end of Valles Marineris may be indicative of major changes in crustal properties associated with faulting or the removal of magnetic material from this region. An apparent offset or truncation of this same feature occurs at Ganges Chasma (G on Plate 1), north of Valles Marineris. Additional inversions and forward modeling will be required to establish the directions of magnetization in this region before detailed interpretation can proceed. The altitude-normalized map and associated materials are available in digital form from the authors' web site (http://denali.gsfc.nasa.gov/research /purucker/mars_mag.html).

While most (and certainly the strongest) magnetic features are located in old terrain south of the crustal dichotomy boundary, some significant magnetic features are found north of the boundary, in young, sparsely cratered plains, especially west of Olympus Mons, and in eastern Chryse. If, as most believe, the core field of Mars shut off early, these younger regions may represent thin cover over ancient terrains magnetized while the main field was still present.

Reduction to a common altitude reinforces the appearance of symmetry of maximum magnetic fields in the Terra Cimmeria and Serenum regions. *Connerney et al.* [1999] have interpreted the long linear magnetic features here as a possible signature of plate tectonic processes though other processes are also plausible.

These initial results from the altitude-normalized magnetic map (e.g. laterally offset anomalies at G and truncated at V) show that interpretation of this data set will have a major influence in understanding not only the ancient, but also the more modern tectonics of Mars.

References

Acuña, M., J. Connerney, N. Ness, R. Lin, D. Mitchell, C. Carlson, J. McFadden, K. Anderson, H. Rème, C. Mazelle, D. Vignes, P. Wasilewski, and P. Cloutier, Global distribution of crustal magnetization discovered by the Mars Global Surveyor MAG/ER experiment, *Science*, *284*, 790-793, 1999.

Acuña, M., Digital, layered map of Mars crustal magnetization, http://mgs-mager.gsfc.nasa.gov/, 1.4 Mb, 2000

Blakely, R.J., R. Wells, T. Yelin, I. Madin, and M. Beeson, Tectonic setting of the Portland-Vancouver area, Oregon and Washington: Constraints from low-altitude aeromagnetic data, *Geol. Soc. Amer. Bull.*,*107*,1051-1062, 1995.

Connerney, J., M. Acuña, P. Wasilewski, N. Ness, H. Rème, C. Mazelle, D. Vignes, R. Lin, D. Mitchell, and P. Cloutier, Magnetic lineations in the Ancient Crust of Mars, *Science*, *284*, 794-798, 1999.

Purucker, M., T. Sabaka, and R. Langel, Conjugate gradient analysis: A new tool for studying satellite magnetic data sets, *Geophys. Res. Lett.*, *23*, 507-510, 1996.

Zuber, M., S. Solomon, R. Phillips, D. Smith, G. Tyler, O. Aharonson, G. Balmino, W. Banerdt, J. Head, C. Johnson, F. Lemoine, P. McGovern, G. Neumann, D. Rowlands, and S. Zhong, Internal structure and early thermal evolution of Mars from Mars Global Surveyor topography and gravity, *Science*, *287*, 1788-1793, 2000.

M. Acuña, Code 691, Goddard Space Flight Center, Greenbelt, MD 20771

H. Frey, M. Purucker, T. Sabaka, C. Voorhies, Code 921, Goddard Space Flight Center, Greenbelt, MD 20771. (e-mail:purucker@geomag.gsfc.nasa.gov)

D. Ravat, Dept. of Geology, Southern Illinois University, Carbondale, IL 62940